



Contents lists available at ScienceDirect

## Journal of Sound and Vibration

journal homepage: [www.elsevier.com/locate/jsvi](http://www.elsevier.com/locate/jsvi)

# Minimax design of vibration absorbers for linear damped systems

Brandon Brown, Tarunraj Singh \*

*Department of Mechanical and Aerospace Engineering, State University of New York at Buffalo, Buffalo, NY 14260, United States*

## ARTICLE INFO

*Article history:*

Received 11 August 2010

Received in revised form

30 November 2010

Accepted 1 December 2010

Handling Editor: K. Worden

## ABSTRACT

This paper addresses the issue of design of a passive vibration absorber in the presence of uncertainties in the forcing frequency. A minimax problem is formulated to determine the parameters of a vibration absorber which minimize the maximum motion of the primary mass over the domain of the forcing frequency. The limiting solutions corresponding to the forcing frequency being unrestricted and to that where the forcing frequency is known exactly, are shown to match those available in the literature. The transition of the optimal vibration absorber parameters between the extreme two cases is presented and the solutions are generalized by permitting the mass ratio of the absorber mass and the primary mass to be design parameters. For the specific case where the primary system is undamped, detailed analysis is presented to determine the transition of the optimal vibration absorber parameters between three distinct domains of solutions.

© 2010 Elsevier Ltd. All rights reserved.

## 1. Introduction

A vibration absorber is a passive device which is designed to limit the vibration of a main structure and has been used to retrofit buildings with unacceptable vibrations [1], in reducing the chatter in turning operations [2] and for damping the wind excited motion of transmission line towers [3]. Since the vibration absorber was introduced in 1909 by Frahm [4], there has been much work on the optimization of the design and tuning of the vibration absorber. Most optimizations are concerned with the classic vibration absorber model, which neglects damping in the protected structure.

The first optimization of the single degree of freedom (DOF) classic model vibration absorber was offered in closed form by Den Hartog [5], where an analytical solution for the frequencies corresponding to the two maxima of the frequency response function is determined. In an effort to minimize the maximum vibration of the main mass, the frequency response magnitude at these points is set equal. Warburton [6] extended this work on the classical single DOF vibration absorbers to multiple DOF systems. Current work has evolved from applying single DOF methodologies to multiple DOF, to unique techniques for multiple DOF systems [7]. Optimization techniques have also been developed for more complex single DOF vibration absorber models. Viguié et al. [8] developed a method of using a frequency energy plot to optimize a damped nonlinear single DOF absorber attached to a damped main mass with a nonlinear stiffness. The concept of vibration absorbers for lumped mass systems has been extended to distributed parameter systems, e.g., for the control of beam using piezoelectric patches [9]. Additional flexibility has been added to traditional vibration absorbers by permitting the coefficient of stiffness and damping to be varied, resulting in a semi-active vibration absorber [10,11].

Randall [12] developed a method which minimized the maximum vibration magnitude of the damped main mass in a single DOF system. This method selects the maximum magnitude of the two resonance magnitude peaks and creates a surface of this magnitude as a function of the vibration absorber design variables. The optimal solution is then found using a Golden

\* Corresponding author.

*E-mail addresses:* [brbrown@buffalo.edu](mailto:brbrown@buffalo.edu) (B. Brown), [tsingh@buffalo.edu](mailto:tsingh@buffalo.edu) (T. Singh).

Section grid search. This method will not arrive at the optimal solution since it cannot create a system where the two resonance peaks are of the same magnitude. Pennestrì [13] exploits the Chebyshev Equioscillation Theorem which states that the polynomial of the best approximation overestimates and underestimates the function to be approximated at least  $n+2$  times when a  $n$ th order polynomial is used as the approximating function. For the two degree of freedom system, the frequency response function is characterized by three stationary points which correspond to two maxima and one minima. An optimization problem which minimizes the maximum motion of the primary mass subject to the six constraints derived from the Chebyshev Equioscillation Theorem is solved to determine the parameters of a vibration absorber which is robust to uncertainties in forcing frequencies. Kwak et al. [14] developed a steepest descent minimax method for the classical vibration absorber model. They illustrate the performance of the vibration absorber for three sets of design constraints which include the *rattle space* constraint which limits the relative motion of the primary and absorber masses. In contrast to the steepest descent approach, Viana et al. [15] use the ant colony optimization approach, a probabilistic technique to arrive at the optimal parameters of a vibration absorber.

The focus of this paper is on the formulation of a minimax optimization problem which minimizes the maximum displacement of the primary mass over a range of forcing frequencies. Following the presentation of the dynamics of the vibration absorber in Section 2, an unconstrained minimax optimization problem is formulated in Section 3, which minimizes the maximum magnitude of motion of the primary mass over a domain of uncertain forcing frequency. In Section 4, the results of the minimax optimization problem are presented and compared to those presented by Pennestrì [13]. In this section, the damping and the spring stiffness of the absorber are the optimization variables and it is shown that the Pennestrì results are optimal only for systems where the uncertainty in the forcing frequency is large. The optimal absorber parameters are presented as a function of the range of forcing frequency to illustrate the benefit of using the minimax optimization problem to determine the parameters of the vibration absorber. In the penultimate section, the inclusion of the mass ratio in the set of variables to be optimized for and the effect of damping of the primary system on the design of the vibration absorber are presented which provides a new insight into the design and the performance of the vibration absorbers as a function of primary mass damping ratio and mass ratio of the primary and absorber masses.

## 2. Vibration absorber equations of motion

The vibration absorber model used in this paper is shown in Fig. 1. The dynamics of the primary mass ( $m_1$ ) and the absorber mass ( $m_2$ ), subject to a sinusoidal forcing on the main mass, are given by the equations:

$$m_1\ddot{x}_1 = b_2(\dot{x}_2 - \dot{x}_1) + k_2(x_2 - x_1) - b_1\dot{x}_1 - k_1x_1 + F_1 \sin(\omega t), \quad (1)$$

$$m_2\ddot{x}_2 = b_2(\dot{x}_1 - \dot{x}_2) + k_2(x_1 - x_2). \quad (2)$$

The sinusoidal response of the two masses after the transients have died out is given by the equations:

$$x_1 = X_1 \sin(\omega t + \psi_1), \quad (3)$$

$$x_2 = X_2 \sin(\omega t + \psi_2). \quad (4)$$

The maximum displacement of the vibration absorber relative to the primary mass is

$$X_r = X_2 - X_1. \quad (5)$$

The objective of the vibration absorber is to minimize the vibration of the primary mass. The optimization problem formulated in this work endeavors to minimize the maximum vibration magnitude of the primary mass. From the system dynamic equations, an expression for the maximum displacement of the main mass,  $X_1$ , is developed. An expression for the maximum displacement magnitude between the vibration absorber mass and the primary mass,  $X_r$ , is also developed.

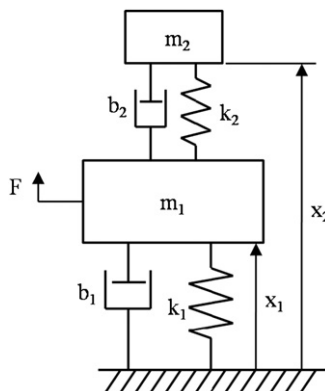


Fig. 1. Vibration absorber system.

In order to make this a general approach, generalized coordinates will be used to describe the displacement of the masses in the system. Notation used by Pennestrì [13] and earlier by Randall [12] is utilized in this development.

$$\alpha = \frac{k_1 X_1}{F} = Z^{-1} \sqrt{(1 - \beta^2 T^{-2})^2 + 4(\zeta_2 \beta T^{-1})^2}, \tag{6}$$

$$\gamma_r = \frac{k_1 X_r}{F} = Z^{-1} \beta^2 T^{-2}, \tag{7}$$

where  $\alpha$  is the normalized maximum displacement of the main mass,  $\gamma_r$  is the normalized maximum relative displacement of the vibration absorber mass, and  $Z^2$  and the normalized variables are defined as

$$Z^2 = [\beta^4 T^{-2} - \beta^2 T^{-2} - \beta^2(1 + \mu) - 4(\zeta_1 \zeta_2 \beta^2 T^{-1}) + 1]^2 + 4[\zeta_1 \beta^3 T^{-2} + \zeta_2 \beta^3 T^{-1}(1 + \mu) - \zeta_2 \beta T^{-1} - \zeta_1 \beta]^2, \tag{8}$$

$$\omega_i = \sqrt{\frac{k_i}{m_i}}, \zeta_i = \frac{b_i}{2\sqrt{k_i m_i}}, \beta = \frac{\omega}{\omega_1}, T = \frac{\omega_2}{\omega_1}, \mu = \frac{m_2}{m_1}. \tag{9}$$

It can be seen that the displacement magnitude is a function of five variables:  $\beta$ ,  $\zeta_1$ ,  $\zeta_2$ ,  $\mu$  and  $T$ . The normalized forcing frequency,  $\beta$ , is an unknown input to the system. The damping ratio of the main mass,  $\zeta_1$ , is a specified variable of the protected system. Thus there are three variables which can be selected by the designer to minimize the vibration of the main mass. The absorber mass ratio,  $\mu$ , is likely to be specified by a design but may be a free variable for the vibration absorber design. In the very least  $\mu$  will have bounds for the vibration absorber design. There are two variables which can be selected by the vibration absorber designer to tune the performance of the absorber: the vibration absorber damping ratio ( $\zeta_2$ ) and frequency ratio ( $T$ ). In some situations the vibration absorber mass ratio ( $\mu$ ) becomes a third design variable. In the first part of this work an optimal  $T$  and  $\zeta_2$  will be found for a specified mass ratio, for varying normalized forcing frequency ranges. Once the solution is found for a specific mass ratio, it will be investigated how the vibration absorber mass ratio affects the maximum displacement magnitude, and optimal designs will be found for each combination of mass ratio and forcing frequency range. The effects of the main system damping ratio on the optimal vibration absorber will also be studied.

### 3. Minimax optimization formulation

In most systems, the frequency of the external disturbances are not known exactly. An ideal vibration absorber will perform well over a range of possible external forcing frequencies. Pennestrì [13] has developed a method which uses Chebychev's min-max criterion to arrive at the optimal parameters of a vibration absorber. The resulting absorber is the optimal solution if forcing frequency varies over a large range. The domain of the uncertain forcing frequency is not exploited in the design process. One can conjecture that if information about the range of forcing frequencies is included in the design of the absorber, improvements in the performance of the absorber can be attained. A minimax optimization of the maximum main mass displacement over the range of the uncertain frequency offers this advantage. The minimax optimization finds the values of design variables which minimize the maximum cost function value over a given range of a set of uncertain parameters. In this vibration absorber design problem, the uncertain parameter is the forcing frequency and the cost function is the normalized maximum displacement of the primary mass. The design variables are the damping ratio and frequency ratio of the vibration absorber subsystem. In some applications it may be desired to constrain the maximum vibration magnitude of the absorber mass as well. In such applications, the optimization problem will include a constraint on  $\gamma_r$ .

The minimax method developed in this paper will perform best when the domain of included forcing frequencies is the smallest (i.e., the uncertainty of the forcing frequency is small). As the range of forcing frequency increases the solution found by the minimax optimizer will converge toward the same solution as Pennestrì's method. If knowledge about the probability distribution of forcing frequencies is known, it can be easily incorporated in the minimax cost function resulting in a minimax problem which minimizes a weighted magnitude of the maximum motion of the primary mass. The optimization problem proposed in this paper can be posed as the minimax problem:

$$\min_{\zeta_2, T} \max_{\beta_L \leq \beta \leq \beta_U} \alpha \tag{10}$$

$$\text{subject to : } |\gamma_r(\beta)| \leq \gamma_{des}. \tag{11}$$

The solution to Eq. (10) will be the  $\zeta_2$  and  $T$  which will minimize the maximum  $\alpha$  over the domain of interest of  $\beta$ , which also satisfies the  $\gamma_r$  constraint.

### 4. Numerical results

The first example considered is to permit a comparison to a previous work [13] which developed an approximate method to the damped main mass vibration absorber problem. This comparison will show the advantage of the proposed method over the frequency range of interest. The second example set illustrates the dependence of the vibration absorber design and performance on the vibration absorber mass ratio and the main system damping ratio.

#### 4.1. Example 1

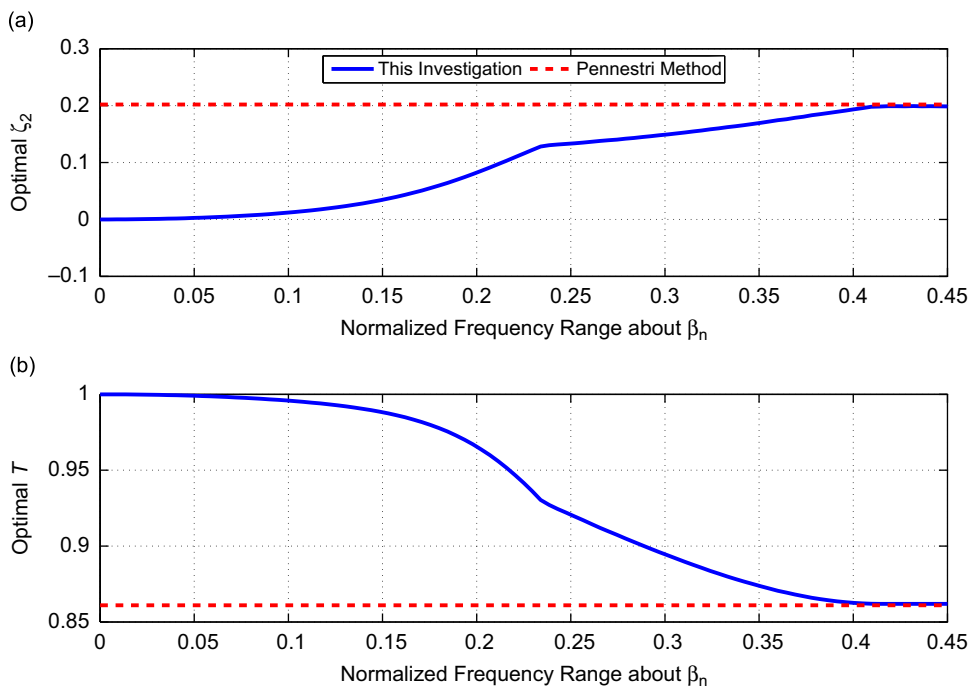
Using the problem formulation proposed in this paper, the non-dimensional parameters of the primary system are  $\mu = 0.1$ ,  $\zeta_1 = 0.1$ , and  $\omega_1 = 100$  rad/s. The nominal forcing frequency was selected to be the natural frequency of the main system ( $\beta_n = 1$ ) and the frequency range of interest was centered on this frequency. No additional knowledge of the forcing frequency distribution is utilized in these results. For this set of solutions there was no limit set on the absorber mass vibration magnitude,  $\gamma_{des}$ . It can be seen in Fig. 3 that the solution to the problem posed in this paper performs better than those presented by Pennestri [13], when the range of the forcing function frequency is small. When the normalized frequency range around the nominal frequency remains below 0.405, the method developed offers a significant advantage. The minimax approach presented in this paper outperforms the previous work [13] below a frequency range of 0.405 since the two resonance peaks are not included in the domain of interest and consequently the optimizer is not constrained by magnitude of the resonance peaks. Converting to standard frequencies, a 0.405 normalized range relates to a forcing frequency range of  $82.8 \text{ rad/s} \leq \omega \leq 117.2 \text{ rad/s}$ . As the range of the forcing function frequency increases, the solution asymptotically approaches that presented in the paper by Pennestri [13]. If the frequency range of interest do not include the two resonance peak frequencies then the proposed method would yield even larger improvements over a non-specific frequency range method. Notice in Table 1 that the reported  $\gamma_{max}$  value does not exactly match that presented in [13].

Fig. 2 illustrates the optimal parameters of the vibration absorber as the range of the frequency about the nominal forcing frequency increases. Notice in Figs. 2 and 3 around the frequency range of 0.23, the optimal parameters transition sharply. These points are where the first resonance peak enters the range of interest of the forcing frequency. It should also be noted in Figs. 2 and 3 that  $\alpha_{max}$  for a normalized frequency range of 0 which corresponds to exact knowledge of the forcing frequency results in a zero displacement of the primary mass and the corresponding damping ratio of the absorber is zero, which is the expected result. In Figs. 2 and 3 the Pennestri solution is considered constant. The value for  $\alpha_{max}$  was evaluated over varying ranges of forcing frequency for the Pennestri solution, but the solution varied only slightly. This slight variation can be seen in Fig. 4, as the small difference between the minima and the maxima over the larger frequency ranges. Fig. 4 illustrates the evolution of the optimal  $\alpha$  curve as a function of the forcing frequency range. In this figure the surface is plotted over the range

**Table 1**

Example 1: Optimal parameters.

	$T_{opt}$	$\zeta_{2,opt}$	$\alpha_{max}$	$\gamma_{max}$
<b>Pennestri</b>	0.861	0.202	2.6272	6.1883
<b>This investigation</b>	0.8619	0.1986	2.6227	6.2488



**Fig. 2.** (a) Optimal  $\zeta_2$ . (b) Optimal  $T$ .

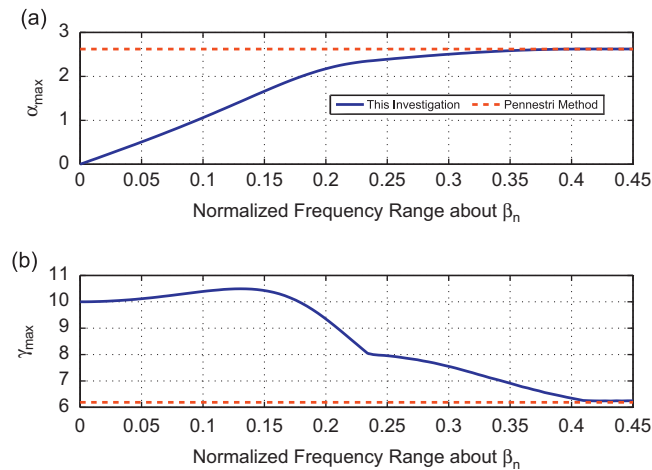


Fig. 3. (a) Optimal  $\alpha_{\max}$ . (b) Optimal  $\gamma_{\max}$ .

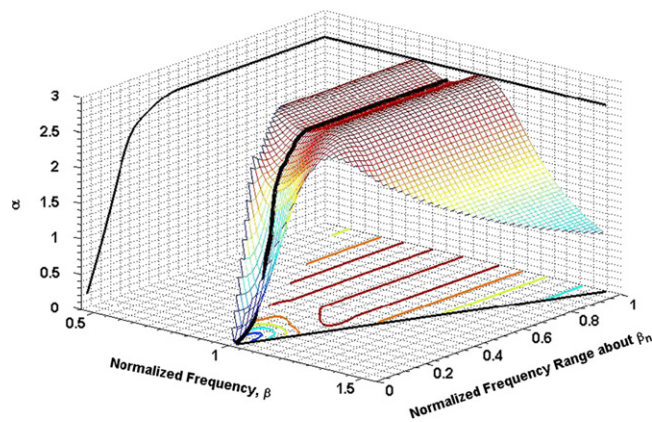


Fig. 4. Variation of maximum normalized displacement vs. frequency.

of permitted forcing frequency. It can be seen as the range of normalized frequency range increases from zero,  $\alpha$  starts at zero and saturates at a value which corresponds to Pennestri [13] solution which is valid for an unconstrained range of forcing frequency. A solid black line is included in the valley of surface to illustrate the movement of the minima of the surface to smaller values of  $\beta$  as the frequency range is increased.

For all of this study the frequency range of interest varied from 0 to 0.45. The upper limit of 0.45 was selected since this was larger than the range at which the optimal parameters of the absorber do not change. The lower limit of 0 was selected to illustrate the behavior of the vibration absorber design at a known frequency. At a known frequency an optimal vibration absorber will be one which has the same natural frequency as the main system with no damping. This vibration absorber design will result in exactly zero vibration of the main mass and a  $\mu^{-1}$  maximum magnitude vibration of the absorber mass. All of these expected results were confirmed by the results and are shown in Figs. 2 and 3.

## 5. Example 2

In this section, the proposed minimax approach is used to study the effect of the main mass system damping ratio,  $\zeta_1$ , and the mass ratio,  $\mu$ , on the optimal vibration absorber parameters.

### 5.1. Effect of $\zeta_1$

In this subsection the effects of the main system damping ratio on the optimal design of a vibration absorber are studied. Results illustrated in Figs. 2 and 3 can be generalized by including an additional dimension which corresponds to the damping ratio of the primary system. Figs. 5 and 6 show the effects of main mass damping on the optimal maximum values of  $\alpha$  and  $\gamma_r$ . Figs. 7 and 8 illustrate the sensitivity of the design variables to the main mass damping. The vibration absorber in these figures has a mass ratio of 0.1 ( $\mu = 0.1$ ).

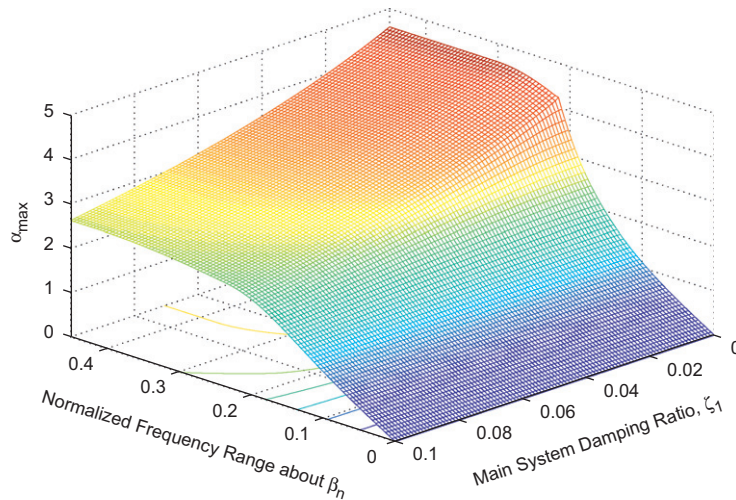


Fig. 5. Damping ratio study: optimal  $\alpha_{\max}$ .

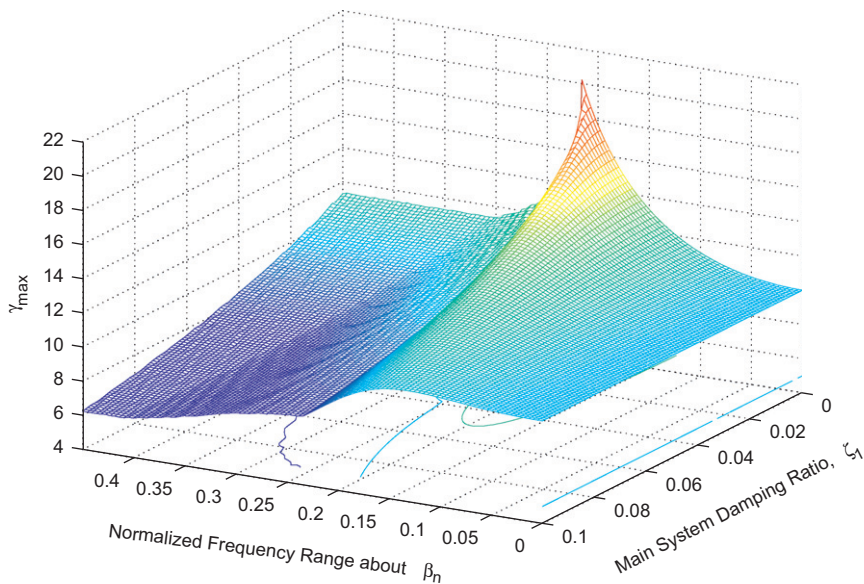


Fig. 6. Damping ratio study: optimal  $\gamma_{\max}$ .

Notice in Fig. 5 that the maximum mass vibration magnitude has three distinct sensitivity domains: at small and large frequency ranges and at a narrow band in between. Fig. 6 shows a spike in the maximum vibration absorber magnitude along a frequency range ridge of 0.216. This coincides with the inclusion of the first resonance peak in the range of interest. Fig. 7 illustrates the variation of the optimal  $\zeta_2$  as a function of frequency range and  $\zeta_1$ . The relatively smooth transition seen in Example 1 (Fig. 2) as the frequency range increases for  $\zeta_1 = 0.1$ , can be seen in Fig. 7. However, as  $\zeta_1$  decreases the corners in the curve become sharper until at  $\zeta_1 = 0$ , a jump occurs in the optimal value of  $\zeta_2$  when the higher resonance peak is included within the frequency range. The variation of the optimal absorber parameters for  $\zeta_1 = 0$  will be analyzed in greater detail later in this section. The optimal absorber parameters  $\zeta_2$  and  $T$  surfaces show that in some cases very small changes in the frequency range magnitude can cause large changes in the optimal design, especially as the main mass damping decreases.

To better comprehend the results of the minimax optimization, the variation in the parameters of the vibration absorber are studied for systems where the primary system damping ratio  $\zeta_1 = 0$ . It can be seen from Fig. 9(a) that for systems where the primary system's damping ratio is zero, the frequency response function of the vibration absorber system is characterized by two points  $P$  and  $Q$  which are invariant to  $\zeta_2$ . The frequency response function with  $\zeta_2 = 0$ , always lies below the frequency response function for any non-zero value of  $\zeta_2$ . This implies that if the uncertain forcing frequency lies within the frequencies corresponding to the points  $P$  and  $Q$ , the optimal magnitude of the parameter  $\zeta_2$  is zero. For  $\zeta_1 = 0$ , this is evident in Fig. 7 which illustrates the variation of  $\zeta_2$  as a function of the normalized frequency range. Fig. 9(a) also illustrates that the slope of the  $\alpha$

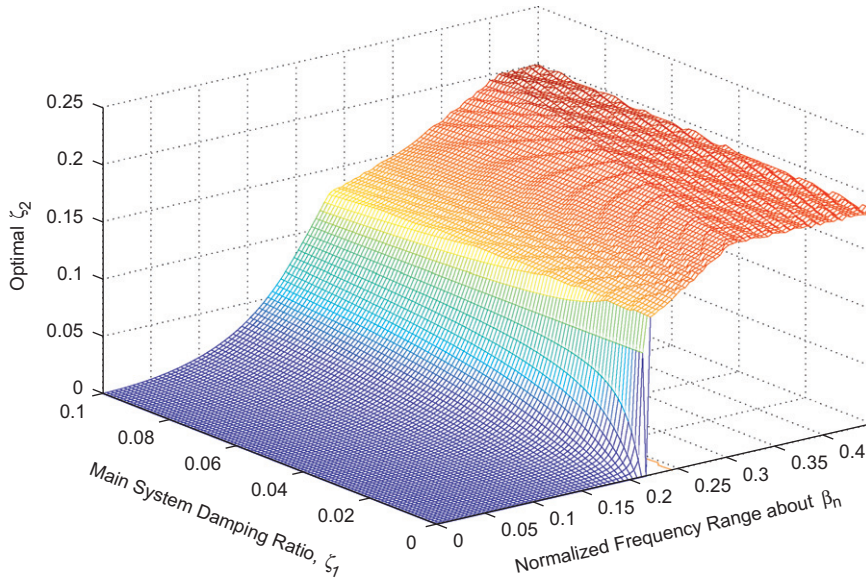


Fig. 7. Damping ratio study: optimal  $\zeta_2$ .

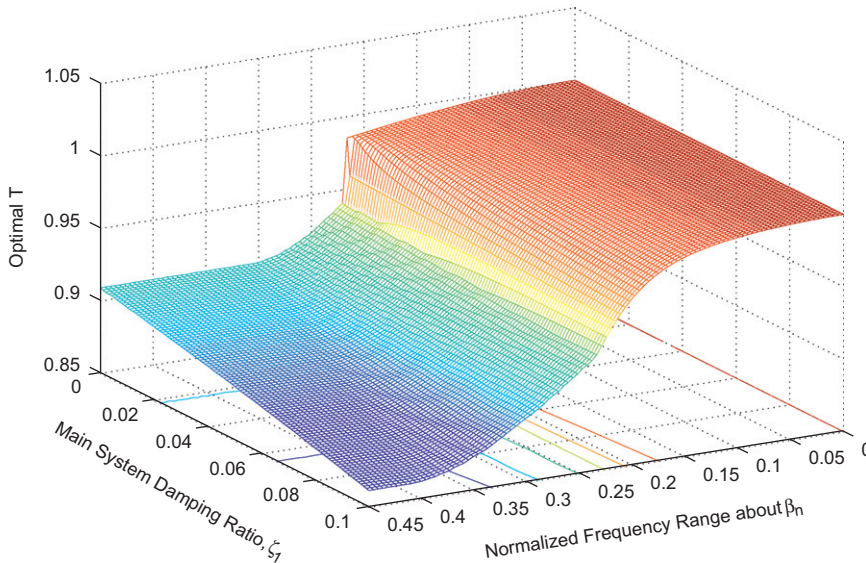


Fig. 8. Damping ratio study: optimal  $T$ .

curve is greater for frequencies which lie below the notch at  $\beta=1$  compared to frequencies above  $\beta=1$ . Note that the notch occurs at  $\beta=T$ . Consequently, for symmetric uncertainty about the normalized frequency of  $\beta=1$ , reducing  $T$  permits equating the worst magnitude of  $\alpha$  at the boundary of symmetric uncertain domain. This intuition is confirmed in Fig. 8 where for  $\zeta_1 = 0$ ,  $T$  gradually decreases with an increase in the normalized frequency range.

Fig. 10 illustrates a sudden change in the frequency response function as the normalized frequency range is increased. This transition occurs when the high frequency resonance peak lies at the border of the uncertain region. The location of this transition is found knowing a few of the characteristics of the transition. First, the frequency response function with and without damping must be equal at both extremes of the range. Second, the slope of the damped frequency response function must be zero at the right ( $Q$ ) point. The exact magnitude of the uncertain region can be determined by simultaneously solving the equations for  $\delta$ ,  $\zeta_t$ ,  $T_0$  and  $T_t$ :

$$\alpha(\beta = 1 + \delta, \zeta = 0, T_0) = \alpha(\beta = 1 + \delta, \zeta = \zeta_t, T_t), \tag{12}$$

$$\alpha(\beta = 1 - \delta, \zeta = 0, T_0) = \alpha(\beta = 1 - \delta, \zeta = \zeta_t, T_t), \tag{13}$$

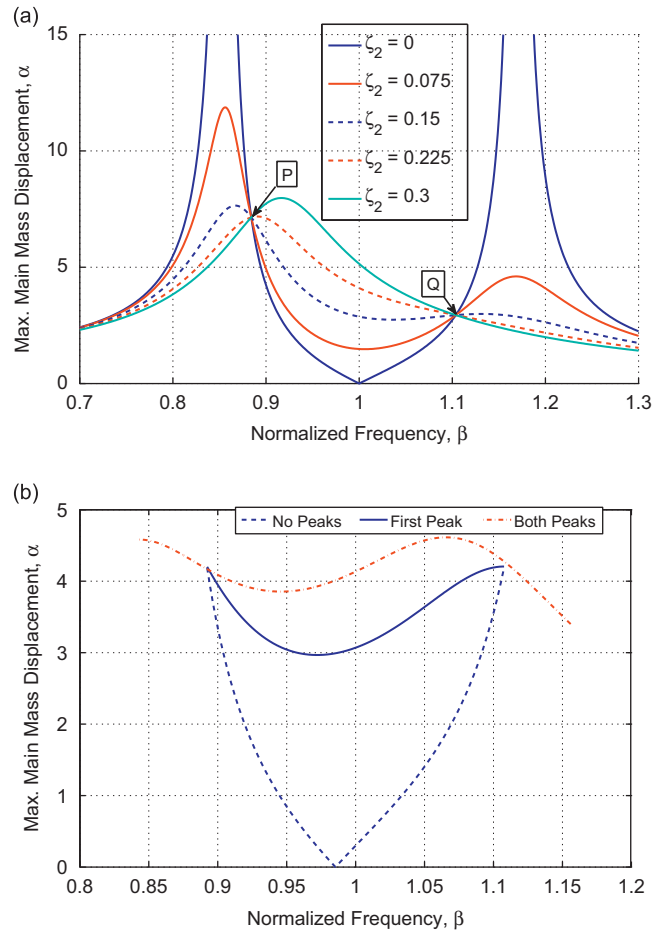


Fig. 9. Classical system frequency response plots: (a) P and Q points and (b) two critical points frequency ranges.

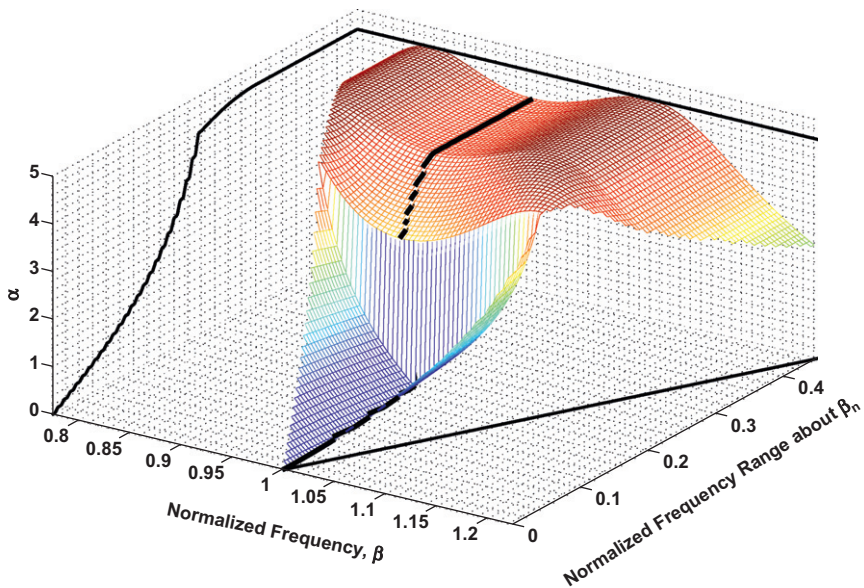


Fig. 10. Variation of maximum normalized displacement vs. frequency.



$$\alpha(\beta = 1 - \delta, \zeta = 0, T_0) = \alpha(\beta = 1 + \delta, \zeta = 0, T_0), \quad (14)$$

$$\frac{d}{d\beta} \alpha(\beta = 1 + \delta, \zeta = \zeta_t, T_t) = 0, \quad (15)$$

where  $T_0$  corresponds to the frequency response curve for  $\zeta_1 = 0$  and  $T_t$  corresponds to the curve for  $\zeta = \zeta_t$ .  $2\delta$  parameterizes the uncertain frequency range which is symmetric about the nominal forcing frequency of  $\beta = 1$ . Using constraint equations, shown in Eqs. (12)–(15), the parameters characterizing the transition of the two frequency response curves are found to be:  $\delta = 0.10781$ ,  $T_t = 0.94218$ ,  $T_0 = 0.98538$ ,  $\zeta_t = 0.13843$ . These values correspond exactly to what is seen in Figs. 7 and 8 before and after the transition to a damped solution. Evaluating the expressions for  $\alpha$  and  $\gamma_r$  at  $\beta + \delta$ , it is found that  $\alpha_{\max} = 4.20576$  and  $\gamma_{\max} = 20.09770$ . These values correspond with the evaluations shown in Figs. 5 and 6.

The solid line in Fig. 9(b) illustrates the frequency response curve at the transition for  $\zeta_1 = \zeta_t$ . The dashed line is the corresponding curve for  $\zeta_1 = 0$ , which illustrates that the magnitude of the two curves are the same the boundary of the uncertain domain of the forcing frequency. The dash-dot line corresponds to the next transition when the two resonance peaks have the same value and the low resonance frequency lies at the lower border of the uncertain frequency domain. After this transition the optimal vibration absorber parameters are invariant to any further increase in the normalized frequency range.

Randall [12] presents analysis of the optimal  $T$  for the case where the primary system damping  $\zeta_1 = 0$ . In Fig. 8, it can be seen for the normalized frequency range greater than 0.3139, the optimal  $T$  is a constant when the damping ratio  $\zeta_1 = 0$ . This corresponds to the case when the two resonance peaks lie within the normalized frequency range and as shown by Randall [12], the optimal value of  $T$  is determined by forcing the magnitudes of the two resonance peaks to be the same and the resulting solution is

$$T = \frac{1}{1 + \mu}, \quad (16)$$

which results in  $T = 0.9091$  for  $\mu = 0.1$ . This is exactly what is shown in Fig. 8 for  $\zeta_1 = 0$ . The closed form expression for the magnitude of the peak is

$$\alpha_{\max} = \frac{2 + \mu}{\mu}, \quad (17)$$

and the two frequencies which correspond to the resonance peaks are

$$\beta_1 = \frac{\sqrt{(2 + \mu)(T^2(\mu + 1) + 1) + \sqrt{T^4(\mu + 1)^2 - 2T^2 + 1}}}{2 + \mu}, \quad (18)$$

$$\beta_2 = \frac{\sqrt{(2 + \mu)(T^2(\mu + 1) + 1) - \sqrt{T^4(\mu + 1)^2 - 2T^2 + 1}}}{2 + \mu}. \quad (19)$$

The frequency range symmetric about  $\beta = 1$  which captures both resonance peaks can be found by the equation:

$$\Delta\beta = 2(\delta) = 2(1 - \beta_2). \quad (20)$$

In Eq. (20),  $\beta_2$  is used since the left resonance peak is the farthest from  $\beta = 1$ . Evaluating Eq. (20) for  $\mu = 0.1$  at the optimal  $T$ , the range is found to be 0.3139. This is exactly what is shown in the results in Fig. 8.

The optimal damping ratio  $\zeta_2$  can be determined from the equation:

$$\alpha(\beta_1) = \frac{2 + \mu}{\mu}, \quad (21)$$

which results in  $\zeta_2 = 0.17779$  which is exactly what is shown in Fig. 7 for a damping ratio  $\zeta_1 = 0$  and for large normalized frequency range.

## 5.2. Effect of $\mu$

This subsection will present the results when the vibration absorber mass ratio is also a design variable. The results of the minimax optimization will yield information about the effects of the selection of mass ratio on the maximum main mass vibration amplitude. Ideally this mass ratio would be as high as possible, but constraints on the system would provide bounds on the acceptable range of mass ratio. The effect of the mass ratio on  $\alpha_{\max}$ ,  $\gamma_{\max}$ , optimal  $\zeta_2$  and optimal  $T$  is shown in Figs. 11–14. The system shown in these figures has a main system damping ratio of  $\zeta_1 = 0.1$ . Notice in each figure that there are regions where small changes in the frequency domain or mass ratio yield large changes in the response/variables of the system. For example, in Fig. 11 it can be seen that if  $\mu$  is increased from 0.1 to 0.25,  $\alpha_{\max}$  can be reduced by almost a third, from 2.2 to 0.75, if the normalized forcing frequency domain range is 0.2. The grid in Fig. 11 is included to illustrate the variation in  $\alpha_{\max}$  for  $\mu$  ranging from near zero to 0.25 in steps of 0.05. The second vertical line and the fifth vertical line correspond to  $\mu$  of 0.1 and 0.25, respectively. Also notice the three distinct domains in Fig. 13, where the optimal  $\zeta_2$  responds very differently to changes in the frequency range and the mass ratio. For small normalized frequency range  $\beta_n$ , and large mass ratio  $\mu$ , the

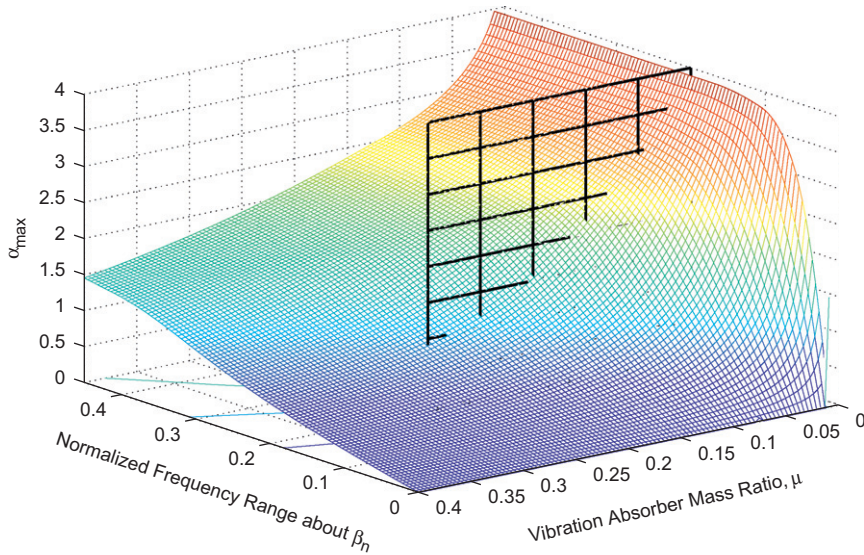


Fig. 11. Mass ratio study: optimal  $\alpha_{\max}$ .

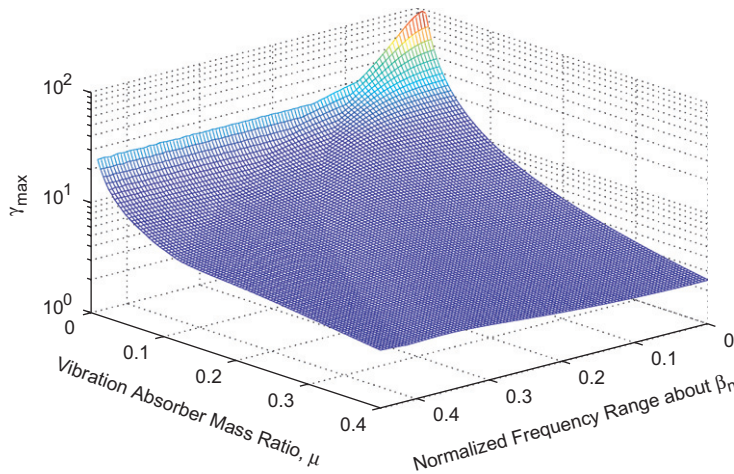


Fig. 12. Mass ratio study: optimal  $\gamma_{\max}$ .

damping ratio of the absorber is small and grows rapidly with a decrease in mass ratio and an increase in the normalized frequency range until it hits a ridge. The growth in the damping ratio of the absorber is slower for further increase in the normalized frequency range and the reduction of the mass ratio. A second ridge highlights the variation of the optimal damping ratio of the absorber for small mass ratio  $\mu$  and large normalized frequency range  $\beta_n$ . The two ridges correspond to the two resonance peaks of the frequency response function of the vibration absorber system influencing the optimal solution of the minimax problem. Fig. 14 also shows a distinct change in the sensitivity of optimal  $T$  to mass ratio and frequency range in the same areas as  $\zeta_2$  (higher frequency ranges). This suggests that the design of the optimal vibration absorber becomes more sensitive to design changes as the range of concerned frequencies increases.

## 6. Conclusions

A minimax problem formulation is presented for the design of parameters for a vibration absorber in the presence of uncertain forcing frequency. This method offers improvement over results presented in the literature by utilizing knowledge about the expected forcing frequency range for a damped main mass system. For the primary system damping  $\zeta_1 = 0.1$ , when the normalized frequency range about the nominal frequency remained below 0.405, this method minimized the maximum main mass displacement magnitude to a value lower than methods available in the literature which do not exploit the frequency ranges of interest in their design. When the range was larger than 0.405 of the normalized frequency, the results of

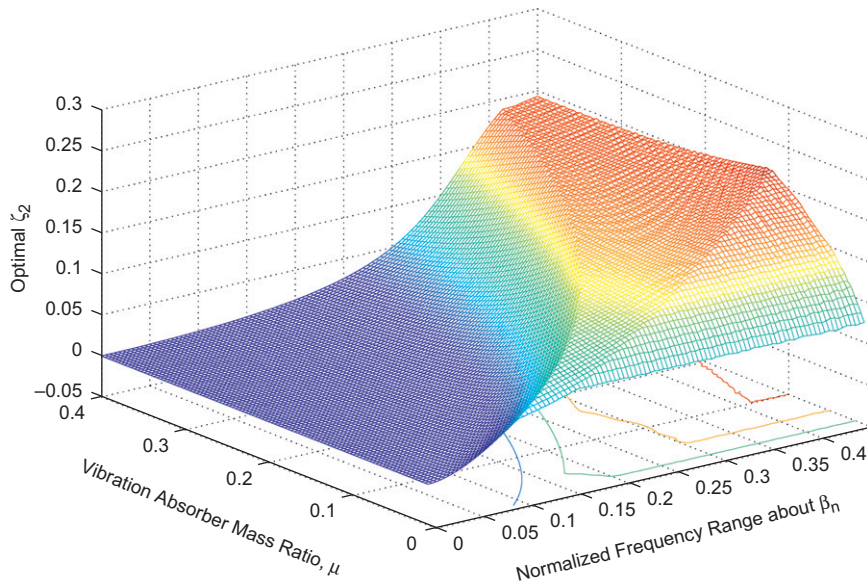


Fig. 13. Mass ratio study: optimal  $\zeta_2$ .

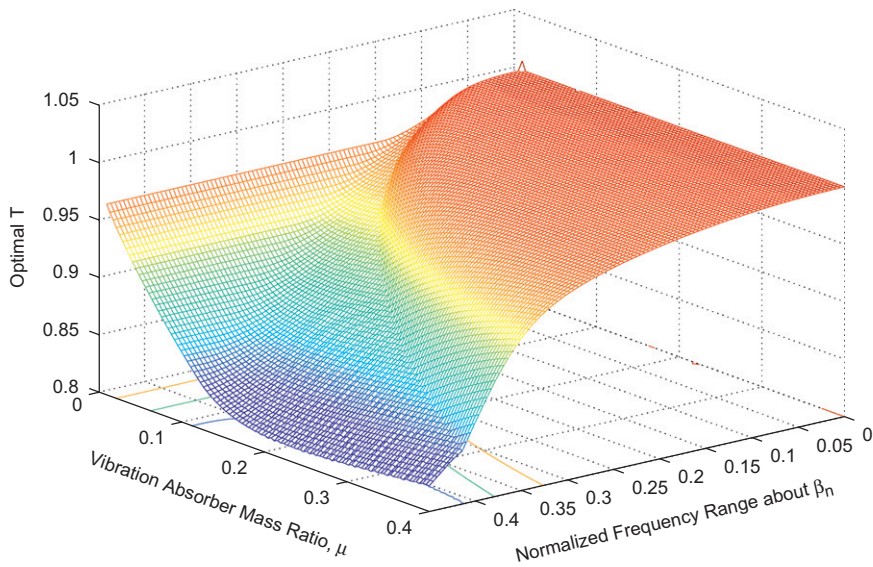


Fig. 14. Mass ratio study: optimal  $T$ .

the proposed method coincided with those available in published papers, offering the advantage of a generalized design approach. The influence of the main system damping on the optimal design and the performance of the vibration absorber was also studied. This study illustrated the extreme sensitivity of the optimal design to slight changes in the forcing frequency range, especially as the main system damping decreases. Results generated for an undamped main system corresponded to expected results of a classical system. The effect of the mass ratio on the performance of the vibration absorber was also studied, illustrating the vibration absorber performance sensitivity to mass ratio, allowing for a more informed decision in the design process. It should be pointed out that the minimax design approach presented in this paper can be extended to deal with multiple absorber design for multi-mode systems and will be carried out in the future.

## References

- [1] A.C. Webster, R. Vaicajtis, Application of tuned mass dampers to control vibrations of composite-floor systems, *Engineering Journal of the American Institute of Steel Construction* 29 (1992).

- [2] Y.S. Tarn, J.Y. Kao, E.C. Lee, Chatter suppression in turning operations with a tuned vibration absorber, *Journal of Materials Processing Technology* 105 (1) (2000) 55–60.
- [3] R.C. Battista, R.S. Rodrigues, M.S. Pfeil, Dynamic behavior and stability of transmission line towers under wind forces, *Journal of Wind Engineering and Industrial Aerodynamics* 91 (8) (2003) 1051–1067 First Americas Conference on Wind Engineering.
- [4] H. Frahm, Device for damping vibrations of bodies, U.S. Patent # 989958, 1911.
- [5] J.P. Den Hartog, *Mechanical Vibrations*, McGraw-Hill, New York, 1956.
- [6] G.B. Warburton, Optimum absorber parameters for minimizing vibration response, *Earthquake Engineering and Structural Dynamics* 9 (1981).
- [7] L. Zuo, S.A. Nayfeh, Minimax optimization of multi-degree-of-freedom tuned-mass dampers, *Journal of Sound and Vibration* 272 (2004).
- [8] R. Vigié, G. Kerschen, Nonlinear vibration absorber coupled to a nonlinear primary system: a tuning methodology, *Journal of Sound and Vibration* 326 (2009).
- [9] J.J. Hollkamp, Multimodal passive vibration suppression with piezoelectric materials and resonant shunts, *Journal of Intelligent Material Systems and Structures* 5 (1) (1994) 49–57.
- [10] N. Jalili, A comparative study and analysis of semi-active vibration-control systems, *Journal of Vibration and Acoustics* 124 (4) (2002) 593–605.
- [11] K. Nagaya, A. Kurusu, S. Ikai, Y. Shitani, Vibration control of a structure by using a tunable absorber and an optimal vibration absorber under auto-tuning control, *Journal of Sound and Vibration* 228 (4) (1999) 773–792.
- [12] S.E. Randall, Optimum vibration absorbers for linear damped systems, *ASME Journal of Mechanical Design* 103 (1981).
- [13] E. Pennestri, An application of chebyshev's mini-max criterion to the optimal design of a damped vibration absorber, *Journal of Sound and Vibration* 217 (4) (1998) 757–765.
- [14] B.M. Kwak, J.S. Arora, E.J. Haug, Optimum design of damped vibration absorbers over a finite frequency range, *AIAA Journal* 13 (4) (1975) 540–542.
- [15] F.A.C. Viana, G.I. Kotinda, D.A. Rade, V. Steffen Jr., Tuning dynamic vibration absorbers by using ant colony optimization, *Computers & Structures* 86 (13–14) (2008) 1539–1549.